Geocarto International

ISSN: 1010-6049 (Print) 1752-0762 (Online) Journal homepage: http://www.tandfonline.com/loi/tgei20

Soil organic carbon mapping using remote sensing techniques and multivariate regression model

Gouri Sankar Bhunia, Pravat Kumar Shit & Hamid Reza Pourghasemi

To cite this article: Gouri Sankar Bhunia, Pravat Kumar Shit & Hamid Reza Pourghasemi (2017): Soil organic carbon mapping using remote sensing techniques and multivariate regression model, Geocarto International, DOI: 10.1080/10106049.2017.1381179

To link to this article: http://dx.doi.org/10.1080/10106049.2017.1381179

Accepted author version posted online: 18 Sep 2017.

Publisher: Taylor & Francis

Journal: *Geocarto International*

DOI: http://doi.org/10.1080/10106049.2017.1381179

Soil organic carbon mapping using remote sensing techniques and multivariate regression model

Gouri Sankar Bhunia[1] , Pravat Kumar Shit[2]*, Hamid Reza Pourghasemi[3]

[1]Manager Aarvee Associates Architects, Engineers & Consultants Pvt Ltd, Hyderabad – 500 082, India.

[2]Department of Geography, Raja N.L.Khan Women's College, Gope Palace, Medinipur-721102, West Bengal, India.

***Email: pravatgeo2007@gmail.com (Corresponding Author)**

[3]Department of Natural Resources and Environmental Engineering, College of Agriculture, Shiraz University, Shiraz, Iran.

Author for Correspondence:

Assistant Professor,

Raja N.L.Khan Women's College,

Department of Geography, Gope Palace,

Medinipur 721102, West Bengal, India

Email: pravatgeo2007@gmail.com

Soil organic carbon mapping using remote sensing techniques and multivariate regression model

Gouri Sankar Bhunia[1] ,Pravat Kumar Shit[2]*, Hamid Reza Pourghasemi[3]

[1]Aarvee Associates Architects, Engineers & Consultants Pvt Ltd, Hyderabad – 500 082, India.

[2]Department of Geography, Raja N.L.Khan Women's College, Gope Palace, Medinipur-721102, West Bengal, India.

[3]Department of Natural Resources and Environmental Engineering, College of Agriculture, Shiraz University, Shiraz, Iran.

***Email: pravatgeo2007@gmail.com (Corresponding Author)**

Abstract

Soil organic carbon (SOC) is an importance aspect of soil quality and plays an imperative role in soil productivity in the agriculture ecosystems. The present study was applied to estimate the SOC stock using space-borne satellite data (Landsat4-5 Thematic Mapper (TM)) and ground verification in the Medinipur Block, Paschim Mednipur District, and West Bengal in India. In total, 50 soil samples were collected randomly from the region according to field surveys using a handheld Global Positioning System (GPS) unit to estimate the surface SOC concentrations in the laboratory. Bare Soil Index (BSI) and Normalized Difference Vegetation Index (NDVI) were explored from TM data. The satellite data derived indices were used to estimate spatial distribution of SOC using multivariate regression model. The regression analysis was performed to determine the relationship between SOC and spectralindices (NDVI and BSI) and compared observed SOC (field measure)to predict SOC (estimated from satellite images). Goodness fit test was performed to determine the significance of the relationship between observed and predicted SOC at $p \leq 0.05$ level. The results of regression analysis between observed SOC and NDVI values showed significant relationship ($R^2 = 0.54$; *P<0.0075*). A significant statistical relationship (r=-0.72) was also observed between SOC and BSI. Finally, our model showed nearly 71% of the variance of SOC distribution could be explained by SOC and NDVI values. The information from this study has advanced our understanding of the on-going ecological development that affects SOC dissemination and might be valuable for effective soil

management.

Keywords: Soil organic carbon; Satellite data; Bare Soil Index; Normalized Difference Vegetation Index, India

1. Introduction

Sustainable land management requires reliable information on the spatial distribution of soil properties affecting both landscape process and services. The concepts of sustainable agriculture put emphasis on the management of soil organic matter for maintaining soil fertility (Shibu et al. 2006). The Soil Organic Carbon (SOC) helps to maintain soil health and productivity. It provides a primary source of nutrients for plants, aids to aggregate particles, develops soil structure, increases water storage capacity, and provides a habitat for soil biota (Schoonover and Crim 2015). Capturing and retaining additional SOC in soil can improve the quality and productivity of the soil to sustain food production and also mitigate the emissions of greenhouse gases (Viscarra Rossel et al. 2016). Maps of SOC is of much interest in agricultural management as well as environmental research related to terrestrial sequestration of atmospheric carbon. Digital mapping of SOC is also important for site specific crop management (Kumar, 2013; Dobermann and Ping 2004).

In conventional soil survey, soil properties are recorded at representative sites and assigned to entire mapping unit, which are delineated through physiographic, physiognomic, and geopedologic approaches. In soil science, vegetation types and condition may be most relevant, in that it reflects and modifies the land surface process such as energy or material exchange modeling (Liu et al. 2011).Although soil surveyors are very well aware of the spatial variability of soil properties, conventionally prepared soil maps do not reflect it as soil units are limited by boundaries (Jaber et al. 2012; Heuvelink and Webster 2001). Naturally, the properties of soil are highly variable (Shit et al. 2015; Burrough 1993) and for accurate estimation of soil properties, these continuous variability should be considered. In the 1970s a new geostatistical technique entitled kriging and its variants were widely recognized as an important spatial interpolation method in land resource inventories (Hengl et al. 2004; Bhunia et al. 2016). The traditional method of soil analysis and interpretation are laborious and time consuming; hence, becoming

expensive. Later in the 1990s, with the advancement of GIS and remote sensing (RS) technology, predictive soil mapping techniques were introduced. Recently, SOC was determined using the visible and infrared channels of hyperspectral images with a field spectrometer to match the spectra of field and satellite images (Gomez et al. 2008; Arrouays et al., 1996). It has also be used in the prediction of SOC (Gupta et al., 2014; Kumar et al. 2016), plant-available soil nutrients, and optimum soil conditions using various spectral indices (Gilabert et al. 2002; Gbolo et al. 2015). These indices are mathematical transformations involving reflectance from different spectral wavelengths.

In India, majority of soil maps were prepared by conventional methods and a very few work has been done so far using modern spatial prediction techniques (Juma et al. 2016; Filho et al. 2013; Somasundaram et al. 2000; Manchanda et al. 2002). The accurate estimation of spatial distribution of soil organic carbon is important in precision agriculture and is one of the bases for decision and policy making. Therefore, research in environmental monitoring, modeling, and precision agriculture need good quality and inexpensive soil data.

The main objective of the study is to develop digital SOC map using remotely sensed environmental indices, included the use of several spectral bands like red, blue, green, and near-infrared (NIR)bands of Landsat Thematic Mapper (TM)data for estimation of vegetation condition and bare soil characteristics. In both instances, multiple regression models were used to predict the digital SOC distribution in the study area.

2. Materials and Method

2.1. Study area

The geographic extent of Medinipur Block is found between latitudes 22˚23′ 45″ - 22˚ 32′ 50″ N and longitudes 87˚05′40″ - 87˚ 31′ 01″ E (Figure 1), and has an area of 323.6 sq. km. The region is a part of residual Chota Nagpur Plateau with undulating relief having gentle slopes and laterite soil. The altitude of the region varies from 0-65m above the mean sea level. The climate of Medinipur is monsoonal type. The temperature of this area ranges from 9˚C - 43˚C with an average annual rainfall of 1470 mm (District Human Development Report: Paschim Medinipur. 2011). The district is predominantly rural in terms population density and agriculture is the main

economic activity in the area.

2.2. Soil sampling collection and analysis

Soil samples were collected randomly at depth of 0-20 cm for the analysis of nutrient status. Coordinate systems of 50 soil sample sites were registered using a handheld Global Positioning System unit (GERMIN ETREX-10).Soil samples were collected from different land use/land cover categories including dense forest (6), degraded forest (5), open forest (5), paddy field (10), agricultural fallow (12), lateritic upland (5), dry fallow (4) and sandy area (3) at depth of 0 – 20cm of the Midnapur Block. SOC concentration was estimated by Walkely-Black Wet oxidation method (Nelson and Sommers 1996; Bao 2000).

2.3. Data collection and processing

Training data set of SOCs were collected during field observations from the period between December 2014 to March 2015 and measurement of organic concentrations were collected through field surveys. Landsat 4-5 TM data (Path/Row: 139/44; Date of Pass: 12/06/2013 was used to estimate the soil carbon. Satellite image for the month of June, the productive month for crop growth was used in this study. This month indirectly provides information on soil properties of specific sites (Peng et al., 2015). Survey of India (SOI) topographical sheets (1:50,000-scale) were used for rectification of satellite data using ERDAS Imagine v9.0 software (Leica Geosystems GIS and Mapping, LLC, Atlanta, GA, USA). The image to map rectification was applied to correct geometrically the Landsat image to the Universal Transverse Mercator (UTM) projection system with World Geodetic System (WGS) 84 Datum and nearest neighbor algorithm. The total root mean square error (RMSE) for the rectification was 0.234 pixels. The linear contrast stretch function used to increase the contrast and clarity of the image. The flow chart of the procedures involved in the preparation of the digital SOC map is represented in Figure 2.

2.3.1. Bare soil index and NDVI

Bare soil refers to the soil uncovered by grass, other live ground covers, woodchips, gravelly and rocky surfaces, artificial turf and/or similar covering. The bare soil index (BSI) is a numerical indicator that combines blue, red, green and near-infrared channel to capture the soil variations.

The BSI value critically liable on the sun angle vicissitudes and soil background that they are as subtle to soil darkening as to vegetation growth. The BSI values of soil was designed to minimize the identified causes by normalizing sunlight and shaded soil differences and minimize the dry and wet soil conditions (Shabou et al., 2015; Kumar et al., 2016). The BSI is calculated from the satellite data using the following equation according to Jamalabad and Abkar (2004):

$$BSI = \frac{[(Red\ channel_4 + Green\ channel_3) - (Red\ channel_4 + Blue\ channel_1)]}{[(Near-infrared_5 + Green\ channel_3) + (Red\ channel_4 + Blue\ channel_1)]} x\ 100 + 100 \quad (1)$$

In the following equation, 100 were added for the elimination of ambiguity. Finally the BSI map was prepared through color tinting process in ArcGIS v9.0 software (Environmental Systems Research Institute, Inc. Redlands, CA, USA).

Consequently, the Normalized Difference Vegetation Index (NDVI) value was estimated using the NIR(Band $_4$) and red channel (Band$_3$) of TM data to determine the condition of vegetation and is an extent of monitoring changes in vegetation. NDVI was calculated through the following equation (Yongnian et al. 2010):

$$NDVI = (B_4 - B_3) / (B_4 + B_3) \quad (2)$$

Where, B_4 is the reflectance of NIR radiation and B_3 is the reflectance of red radiation of Landsat TM data. The value of NDVI is varied from+1 to -1, with positive values indicating vegetative or high reflective surface while negative values indicate non-vegetative or non-reflective surfaces (Gbolo et al. 2015). Negative values can also be associated with the presence of clouds and water. Bare soils, senesced, dry or non-photosynthetic vegetation have lower values due to the equal or almost equal reflectance of both red and NIR radiations. Healthy green vegetation have high values due to the high reflectance of the NIR radiations. The NDVI derived from the Landsat4-5 TM data was used in the prediction of the SOC.

2.4. Statistical analysis and Digital soil mapping

The descriptive statistics values were analyzed using SPSS 17.0 for three variables such as SOC, NDVI, and BSI. We explored the relations between the two explanatory variables (NDVI and BSI) and the independent variable (SOC) by calculating the Pearson's correlation co-efficient in the '*r*' environment. Student's *t*-test (2-tailed) was employed to measure the significance between variables. General linear regression and multivariate regression models were applied to estimate SOC concentration. A goodness fit test was used to determine significant differences between observed and predicted SOC at $P \leq 0.05$ level. The multivariate regression model was fit based on the coefficient of determination R^2 and the residual plots according to the observed and predicted SOC variables. Parameter estimations were calculated by least squares and R^2 values to evaluate the goodness of fit of the built model. For generating the digital SOC map, the formula of multivariate regression analysis was performed in ArcGIS software v9.0 by raster calculator tool for the preparation of the digital SOC map. Multivariate regression analysis was performed to determine the significant predictor variables that affect the distribution of organic carbon.

2.5 Validation analysis:

Prediction accuracy was evaluated according to the RMSE and the R^2 values. The model with the lowest RMSE and highest R^2valueswas considered to be the most applicable or ideal model (Jaber et al. 2012).

3. Results and Discussion

3.1. Descriptive statistics of the SOC, BSI, and NDVI

The descriptive statistics obtained from the three variables SOC, BSI, and NDVI in the study area are presented in Table 1. The mean of BSI, NDVI, and SOC contents were 125.82, 0.32, and 5.02, respectively. The highest and lowest SOC content in the study area was observed in dense forest land and sandy areas, respectively. The NDVI map of the study area is illustrated in Figure 3a. The NDVI values varied from 0.49 to -0.25, with a mean and standard deviation of 0.37 and 0.36, respectively. The NDVI results also showed vigorous vegetation in north-western and central portions of the area while the eastern part is characterized by lower NDVI values (Figure

3). The spatial distribution of SOC observed in the central and northwestern parts of the area correspond to forest cover (Figure 5).The eastern and north-east parts of the study site had medium SOC values, with fallow land and bare surfaces having lower values. The small patches of the southern and eastern parts of the study sites are covered with grass land, alluvium and scrub land, which had minimum SOC values similar to Bhunia et al. (2016).

The BSI map of the study area is illustrated in Figure 3b. It has been calculated that when BSI value is lesser that means, it has a lesser amount of vegetation or the vegetation is negligible. If BSI value is greater that means, there is more bare soil (Kumar et al. 2016). BSI values varied from 9.26 to 254.01, with a mean and standard deviation of 131.98 and 70.88, respectively. The high BSI values were recorded in the central and south-west regions of the study area, whereas low values were recorded in the eastern parts. The Pearson's correlation coefficient (r) between NDVI and BSI showed significant negative relationship (r = -0.67, $P<0.005$). Therefore, low BSI value is related to soil concealed with high vegetation vigor (high or positive NDVI). Conversely, high BSI values were associated with more open and bare soil, senesced or dried vegetation (low NDVI values greater than zero).

3.2. Relation between NDVI and SOC

NDVI showed a statistically significant relationship with observed SOC (r = 0.74, P<0.0075, F = 57.91), as presented in Figure 4a and Table 2. The model defining this relationship is given below:

$$SOC = 0.161 + 0.029 * NDVI \quad (3)$$

3.3. Relation between BSI and SOC

The relationship between observed SOC and BSI is represented in Figure 4. The results show a showed a statistically significant relationship between SOC and BSI (r=-0.72; F = 51.51; $P<0.0000$). A regression analysis was performed between SOC and BSI obtained from the Landsat image is indicated below:

$$SOC = 10.11 - 0.04*BSI \quad (4)$$

The detail of the regression analysis is represented in Table 3. The adjusted R^2 of the linear regression model is 0.50, indicating that nearly 50% of the variance of SOC could be explained by this variable.

3.4. Prediction of SOC

The regression coefficients and significance of the relationship between the variables analyzed are shown in Table 4. The final model used to assess the SOC distribution is as follows:

$$SOC = 4.26 + 11.91*NDVI - 0.02*BSI \quad (5)$$

The final model was highly significant ($F = 57.65$; $P<0.0001$), which showed that NDVI and BSI are associated with SOC concentration. The adjusted $R^2 = 0.71$ indicated that nearly 71% of the variance of SOC distribution could be explained by these two variables. The outcomes also indicated that SOC increases with increasing NDVI and decreasing BSI. Finally, the multiple regression models were fitted into ArcGIS to generate the digital SOC map using raster calculator (see Figure 5). The maximum value of digital SOC map was recorded as 14.83. However, the high concentrations of organic carbon were distributed in the north-west region and some small pockets in the central part of the study area. The region covered by water bodies and sand showed negligible SOC values, approximately zero, distributed in some small pockets in the central and southern part. The SOC concentration in the eastern part was moderately distributed.

3.5. Validation of model

The statistical correlation between predicted and observed SOC values were calculated (R^2= 0.81, *P<0.001*). The model was found to be 81% accurate in predicting the SOC based on conducive or optimum soil condition. The RMSE of the predictive model was 1.11 with amean error of 0.005. Hence, using the linear model, positive correlation between fields estimated SOC values and predicted digital SOC values were detected. The residual plot between the observed

and predicted SOC were diagrammed and the outcome presented that all samples were randomly scattered between both of them (Figure 6). The descriptive statistics obtain from observed and predicted SOC are presented in Table 5. The goodness fit test results revealed there is no significance difference between observed and predicted SOC at $p \leq 0.05$ level of significance. Therefore, the predicted digital SOC map aids to estimate the SOC for each pixel of the satellite image, thus conforming to the points in the fields.

4. Discussion

Nature of land use, intensity of agriculture, and fertilizer sources are key factors accountable for soil characteristics alteration (Kumar et al. 2016). Several intrinsic soil characteristics such as texture and soil pH as well as climatic surroundings might also have important influences on soil characteristics alteration (Mondal et al. 2016). Our primary aim was to use the satellite derived indices (NDVI and BSI) as proxies for vegetation condition and top surface layer for SOC distribution. In the present study, medium resolution satellite data was used to measure different aspect of environmental measure of SOC concentration. In previous studies (Jaber et al., 2012), the concentration of SOC was determined through field surveys and geostatistical modeling (Bhunia et al. 2016; Shit et al. 2016). Most of these earlier studies were based on field observation and conventional survey conducted to measure digital soil map (Marchetti et al. 2012; Ismail & Yacoub 2012; Abdel-Kader 2011).

Organic carbon controls several soil characteristics together with color, nutrient holding capacity, and nutrient turnover and can assist improve soil composition (Ismail and Yacoub, 2012).SOC is a significant source of nutrients for plants. In this circumstance a direct link was established between NDVI and SOC, such that NDVI may be used as a proxy for the prediction of SOC. In our findings, positive and linear relationship between the NDVI and SOC observed; therefore, supporting the hypothesis that green biomass would respond to the same environmental triggers as SOC. Similar observation has been reported by Mondal et al. (2016); Vargas et al. (2008); and Meyfroidt and Lambin (2008).

The complexities of BSI determination may be pertinent to soil scientist when cast-off as a proxy in environmental modeling to delineate areas with favorable SOC concentrations.

Determination of the spatial and temporal variability in BSI may be used as correlative index of SOC meditation (Mondal et al. 2016). However, we found that SOC values were significantly associated with BSI index. High BSI areas were associated with low SOC areas and vice-versa. This result is also in agreement with the earlier study by Kumar et al. 2016 and Mondal et al. 2016.

The linear model was observed to be the ideal model based on the biomass and digital carbon maps produced (Clerici et al. 2016). Linear relationship between predicted and reference values were created and used as models for practical applications (Abdullah 2015). Therefore, the models hinge on linearly on their indefinite parameters to regulate the forecaster variables. Finally, the digital SOC map created was validated using remotely-sensed data with similar reference field observations. However, a vital limitation of our study was sampling of SOC once during single season. Further, future research needs the incorporation of long-term multiple environmental factors to confirm the strength of the SOC assessment using geospatial technology.

5. Conclusion

In this study, we estimated the amount of organic carbon in topsoil using remote sensing images with field data and multivariate regression model. The present study suggested that these two factors (NDVI and BSI) are imperative for the fruitful determination of SOC concentrations. In future, multi-temporal satellite data are required to improve the prediction accuracy of SOC, specifically, when integrated with remote sensing data and ground based observation. Another drawback in this study is the large pixel size (30m) and wide spectral bands. Despite these drawbacks, results of this study supports the hypothesis that remotely-sensed data can be beneficial for investigating indigenous environmental condition where NDVI and BSI can be used as proxies in determining SOC. The information from this study has advanced our understanding of the on-going ecological development that affect SOC dissemination and might be valuable for effective soil management policy implementation.

References

Arrouays D, King C Vion I, Le Bissonnais Y. 1996. Detection of soil crusting risks related to low soil organic carbon contents by using Discriminant analysis on thematic Mapper data. Geocarto International. 4(11): 11-16.

Abdel-Kader FH. 2011. Digital soil mapping at pilot sites in the northwest coast of Egypt: a multinomial logistic regression approach. Egypt J Remote Sens Space Sci. 14 (1): 29–40.

Abdullah L. 2015. Linear Relationship between CO2 Emissions and Economic Variables: Evidence from a Developed Country and a Developing Country. Journal of Sustainable Development. 8(2): 66-72.

Bao SD. 2000. Soil and agricultural chemistry analysis. China Agriculture Press, Beijing. p -495

Bhunia GS, Shit PK, Maiti R. 2016. Comparison of GIS-based interpolation methods for spatial distribution of soil organic carbon (SOC). Journal of the Saudi Society of Agricultural Sciences (in press). http://dx.doi.org/10.1016/j.jssas.2016.02.001

Burrough P. 1993. Soil variability: a late 20th century view. Soils Fertil. 56:529–562.

Clerici N, Rubiano K, Abd-Elrahman A, Hoestettler JMP, Escobedo FJ. 2016. Estimating Aboveground Biomass and Carbon Stocks in Periurban Andean Secondary Forests Using Very High Resolution Imagery. Forests. 7: 138.

District Human Development Report: Paschim Medinipur. Development & Planning Department Government of West Bengal. May, 2011. Available at: http://wbplan.gov.in/HumanDev/DHDR/DHDR_Paschim%20Medinipur.pdf

Dobermann A, Ping JL. 2004. Geostatistical integration of yield monitor data and remote sensing improves yield maps. Agronomy J. 96: 285–297.

Filho B, Osmar, Rizzo, Rodnei, Lepsch, Igo Fernando, Prado, Hélio do, Gomes, Felipe Haenel, Mazza, Jairo Antonio, & Demattê, José Alexandre Melo. 2013. Comparison between detailed digital and conventional soil maps of an area with complex geology. Revista Brasileira de Ciência do Solo. 37(5): 1136-1148.

Gbolo P, Gerla PJ, Vandeberg GS. 2015. Using high resolution, multispectral imagery to assess the effect of soil properties on vegetation reflectance at an abandoned feedlot. Geocarto International 30(7):1-17.

Gilabert MA, González-Piqueras J, García-Haro FJ, Meliá J. 2002. A generalized soil-adjustedvegetation index. Remote Sens Environ. 82:303 -310

Gomez C, Viscarra Rossel RA, McBratney AB. 2008. Soil organic carbon prediction by hyperspectral remote sensing and field vis–NIR spectroscopy: an Australian case study Geoderma. 146: 403–411.

Gupta G, Singh J, Pandey PC, Tomar V, Rani M, Kumar P. 2014. Geospatial strategy for estimation of soil organic carbon in tropical wildlife reserve. In: Srivastava PK, Mukherjee S, Gupta M, Islam T. (Eds.), Remote Sensing Applications in Environmental Research. Society of Earth Scientists Series. Springer International Publishing, pp. 69–83. http://dx.doi.org/ 10.1007/978-3-319-05906-8_5

Hengl T, Rossiter DG, Stein A. 2004. Soil sampling strategies for spatial prediction by correlation with auxiliary maps. Aust J Soil Res. 41(8):1403–1422

Heuvelink GBM, Webster R. 2001. Modeling soil variation: past, present, and future. Geoderma. 100(3–4):269–301.

Ismail M, Yacoub RK. 2012. Digital soil map using the capability of new technology in Sugar Beet area, Nubariya, Egypt. Egypt J Remote Sens Space Sci. 15 (2): 113–124.

Jaber SM, Lant CL, Al-Qinna MI. 2012. Estimating spatial variations in soil organic carbon using satellite hyperspectral data and mapalgebra. International Journal of Remote Sensing. 32(18): 5077-5103

Jamalabad M, Abkar A. 2004. Forest canopy density monitoring, using satellite images. In: XXth ISPRS Congress, Istanbul. pp 12–23.

Juma R, Pőcze T, Kunics G, Sisák I.2016. Application of Digital Soil Mapping Techniques to Refine Soil Map of Baringo District, Rift Valley Province, Kenya. Springer Environmental Science and Engineering. 205-218. Online ISBN-978-981-10-0415-5.

Kumar P, Pandey PC, Singh BK, Katiyar S, Mandal VP, Rani M, Tomar V, Patairiya S. 2016. Estimation of accumulated soil organic carbon stock in tropical forest using geospatial strategy. The Egyptian Journal of Remote Sensing and Space Sciences. 19: 109-123.

Kumar S. 2013. Soil Organic Carbon Mapping at Field and Regional Scales Using GIS and Remote Sensing Applications. Adv Crop Sci Tech. 1:e105. doi:10.4172/2329-8863.1000e105.

Liu Z, Shao M, Wang Y. 2011. Effect of environmental factors on soil organic carbon stocks across the Loess Plateau region, China, Agriculture, Ecosystems and Environment. 142: 182-194.

Manchanda ML, Kudrat M, Tiwari AK. 2002. Soil survey and mapping using remote sensing. Tropical Ecology. 43(1): 61-74.

Marchetti A, Piccini C, Francaviglia R, Mabit L. 2012. Spatial distribution of soil organic matter using geostatistics: a key indicator to assess soil degradation status in central Italy. Pedosphere. 22 (2): 230–242.

Meyfroidt P, Lambin EF. 2008. Forest transition in Vietnam and its environmental impacts. Glob Change Biol. 14: 1–18.

Mondal A, Khare D, Kundu S, Mondal S, Mukherjee S, Mukhopadhyay A. 2016. Spatial soil organic carbon (SOC) prediction by regression kriging using remote sensing data. The Egyptian Journal of Remote Sensing and Space Sciences. http://dx.doi.org/10.1016/j.ejrs.2016.06.004

Nelson DW, Sommers LE. 1996. Total carbon, organic carbon, and organic matter. In: Sparks DL, Page AL et al (eds) Methods of soil analysis, part 3. Chemical methods, vol 5. Soil Science Society of America Book Series, Wisconsin. pp 961–1010.

Peng Y, Xiong X, Adhikari K, Knadel M, Grunwald S, Greve MH.2015. Modeling Soil Organic Carbon at Regional Scale by Combining Multi-Spectral Images with Laboratory Spectra. PLoS ONE. 10(11): e0142295. https://doi.org/10.1371/journal.pone.0142295

Viscarra Rossel RA. Behrens T, Ben-Dor E, Brown DJ, Demattê JAM, Shepherd KD, Shi Z, Stenberg B, Stevens A, Adamchuk V, et al. 2016. A global spectral library to characterize the world's soil. Earth-Science Reviews 155: 198–230.

Schoonover JE, Crim JF. 2015. An introduction to soil concepts and the role of soils in watershed management. Journal of Contemporary Water Research & Education. 154(1):21-47.

Shabou M, Mougenot B, Chabaane ZL, Walter C, Boulet G, Aissa NB, Zribi M. 2015. Soil Clay Content Mapping Using a Time Series of Landsat TM Data in Semi-Arid Lands. Remote Sens. 7(5), 6059-6078.

Shi Y, Baumann F, Ma Y, Song C, Kuhn P, Scholten T, He JS. 2012. Organic and inorganic carbon in the topsoil of the Mongolian and Tibetan grasslands: pattern, control and implications. Biogeosci. Discuss. 9: 1869–1898.

Shibu ME, Leffelaar PA, Van Keulen H, Aggarwal PK. 2006. Quantitative description of soil organic matter dynamics—A review of approaches with reference to rice-based cropping systems. Geoderma. 137: 1–18

Shit PK, Bhunia GS, Maiti R. 2016. Spatial analysis of soil properties using GIS based geostatistics models. Model. Earth Syst. Environ. 2(2): 1-6.

Shit PK, Paira R, Bhunia GS, Maiti R. 2015. Modeling of potential gully erosion hazard using geo-spatial technology at Garbheta block, West Bengal in India. Modeling Earth Systems and Environment 1(2): 1-16.

Somasundaram J., Natarajan S., Mathan K.K., Arunkumar V. 2000. Soil Resource Appraisal In Lower Vellar Basin, Tamil Nadu, India Using Remote Sensing Techniques. International Archives of Photogrammetry and Remote Sensing. Vol. XXXIII, Part B7. Amsterdam.pp, 623 -628.

Vargas R, Allen MF, Allen EB. 2008. Biomass and carbon accumulation in a fire chronosequence of a seasonally dry tropical forest. Glob Change Biol. 14: 109–124.

Yongnian Z, Wei H, Benjamin ZF, Honghui Z, Huimin. 2010. Study on the urban heat island effects and its relationship with surface biophysical characteristics using MODIS Imageries. Geospatial Information Science. 13(1): 1-7.

Table 1 Descriptive characteristics of SOC, NDVI and BSI in Midnapur block

Parameters	Observed SOC	NDVI	BSI
Mean	5.02	0.31	125.82
Standard Error	0.36	0.01	6.44
Median	5.20	0.32	111.00
Mode	4.20	0.15	78.00
Standard Deviation	2.60	0.10	45.96
Kurtosis	-0.71	-1.08	-1.13
Skewness	-0.01	-0.38	0.50
Range	9.60	0.37	148.00
Minimum	0.30	0.12	65.00
Maximum	9.90	0.49	213.00

Table 2 Model output of SOC prediction based on NDVI

Variables	Coefficient (β)	*SE*	95% CI	p>|z
Intercept	0.161	0.021	0.12 – 0.20	<0.001
NDVI	0.029	0.004	0.02 – 0.04	<0.0001

CI - Confidence Interval, SE – Standard Error

Table 3 Model output of SOC prediction based on BSI

Variables	Coefficient (β)	*SE*	95% CI	p>|z
Intercept	10.11	0.75	8.59 – 11.62	0.000
BSI	-0.04	0.01	-0.05 – -0.03	0.000

Table 4 Model output of SOC prediction using NDVI and BSI

Variables	Coefficient (βs) 95% CI	*SE*	T-statistics	p>|z
Intercept	4.26 (0.98 - 7.53)	1.63	2.61	<0.001
NDVI	11.91(5.81 - 17.99)	3.03	3.93	<0.0001
SOC	-0.02 (-0.04 - -0.009)	0.01	-3.41	<0.0001

Table 5 Comparative assessment between observed and predicted SOC in relation to different land use/land cover characteristics

Land use category	Observed SOC		Predicted SOC		P-Value
	Mean	SD	Mean	SD	
Dense forest	8.46	1.11	6.16	1.77	0.002
Degraded forest	5.05	0.95	4.38	1.35	0.04
Open forest	3.51	0.62	3.63	1.07	0.03
Paddy field	2.88	1.19	2.89	1.53	0.07
Agricultural fallow	2.54	0.63	3.19	1.27	0.01
Lateritic upland	1.32	0.65	1.23	0.52	0.06
Dry fallow	0.94	0.62	1.07	0.39	0.03
Sand area	0.36	0.06	0.79	0.13	0.05

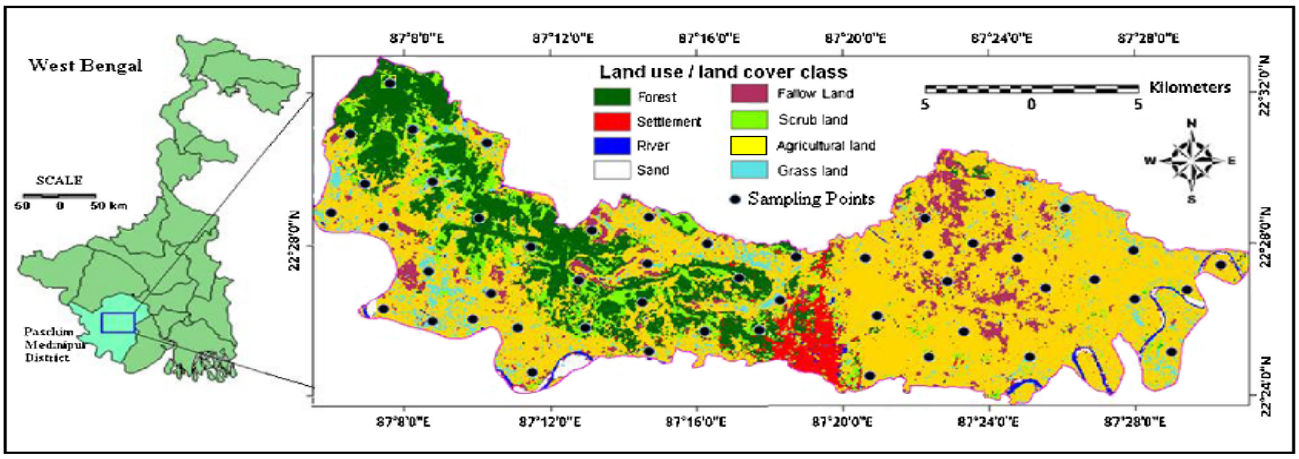

Fig. 1 Location of the study area and sampling sites

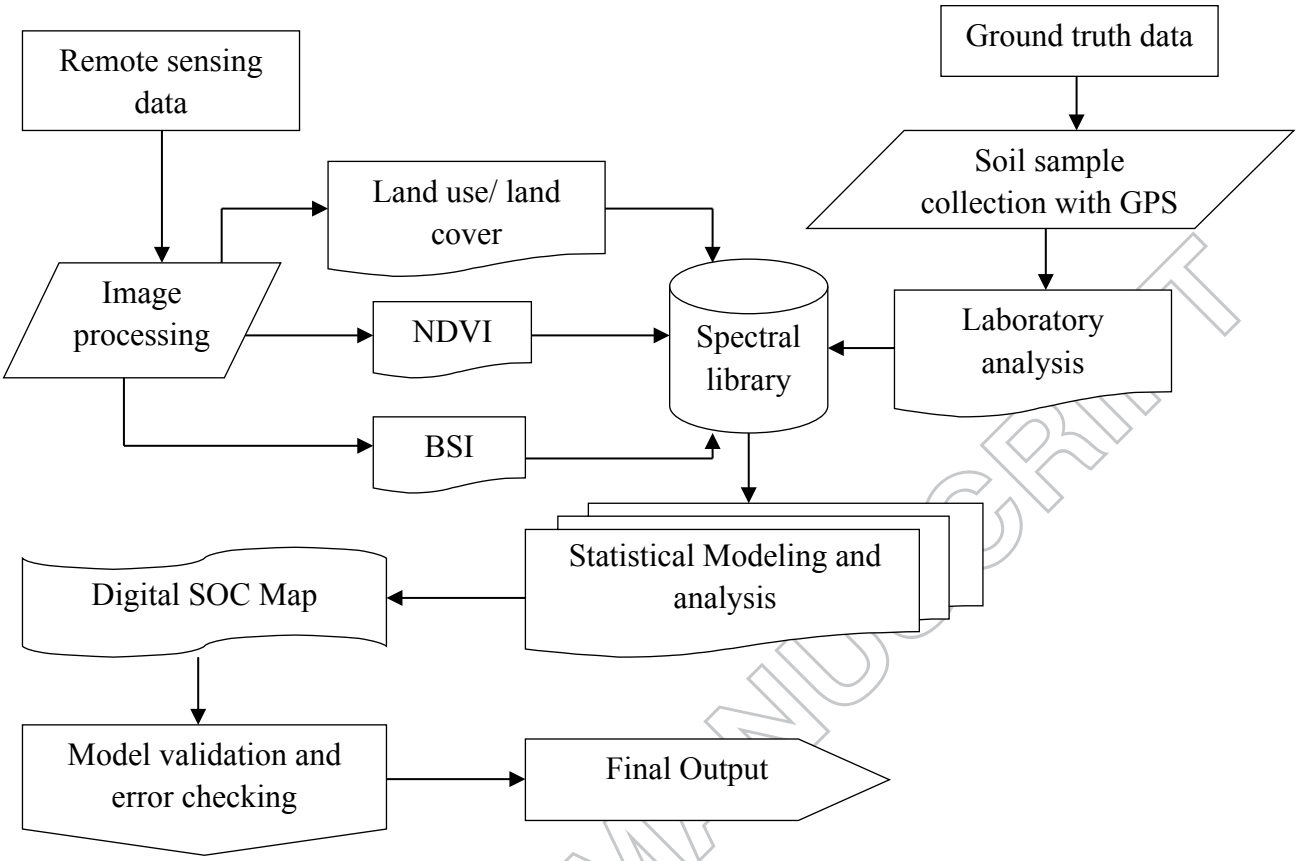

Fig. 2 Flow chart of the methodology

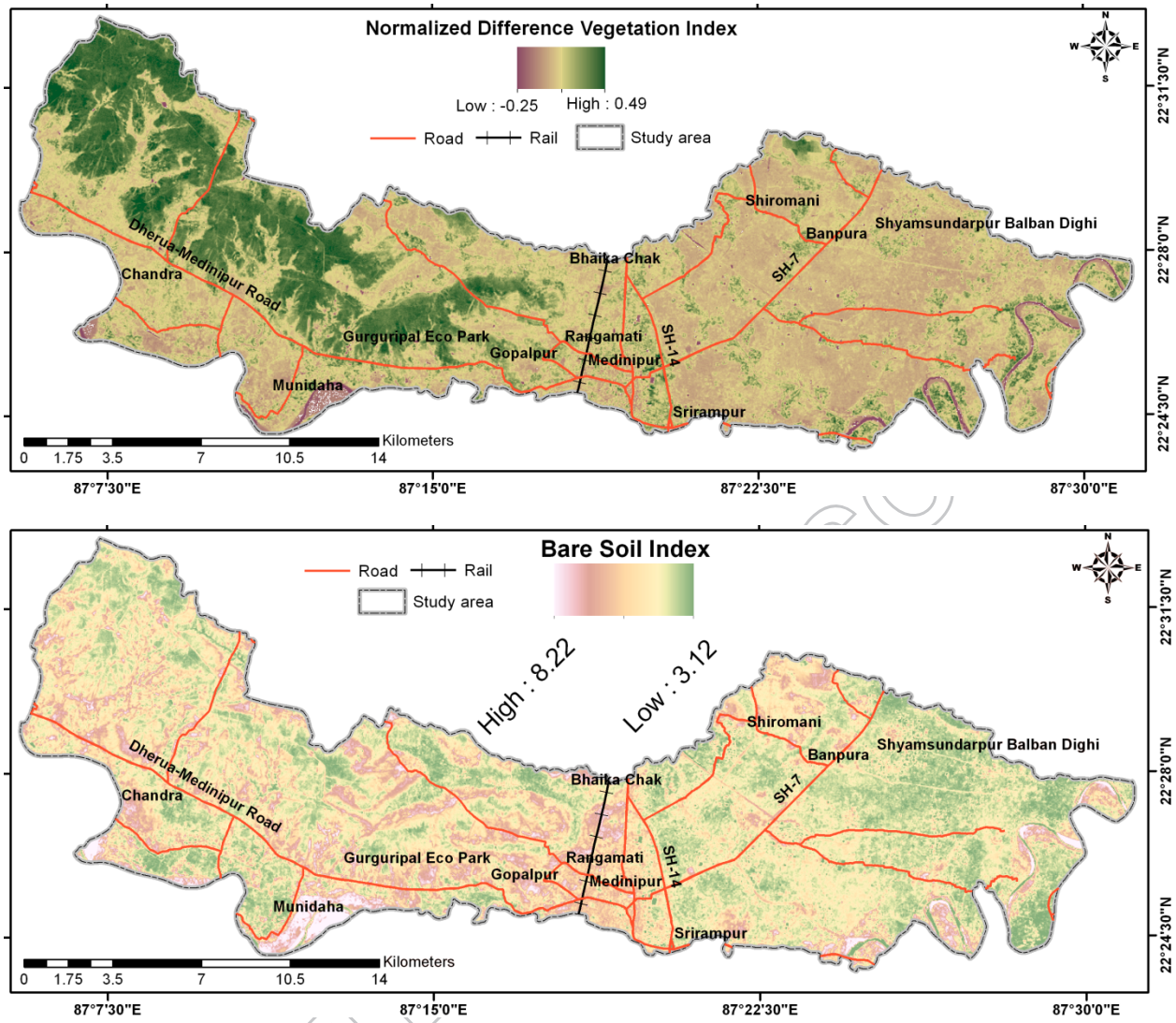

Fig. 3 Spatial distribution of NDVI (a) and BSI maps (b).

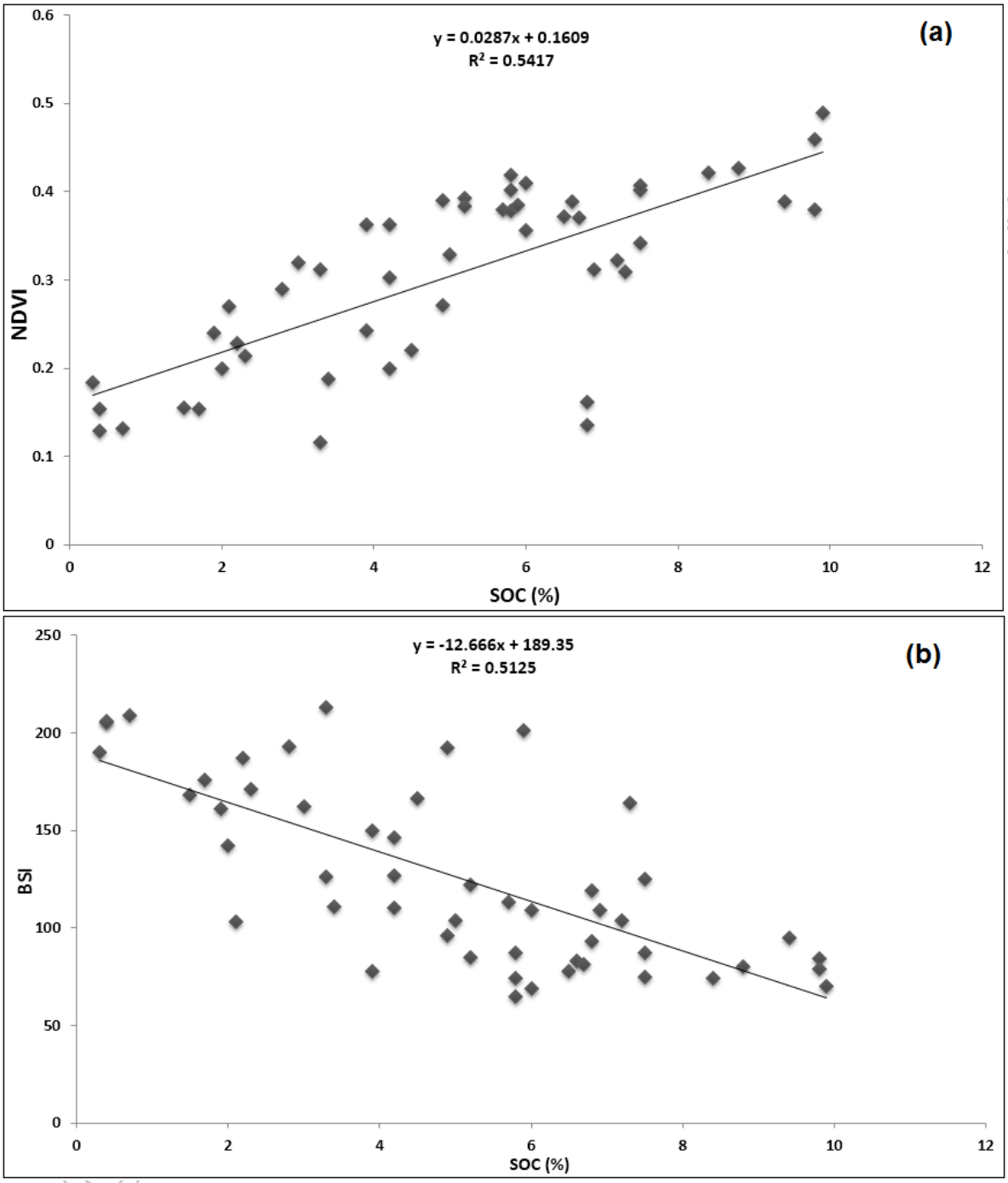

Fig. 4 (a) Association between SOC and NDVI and (b) Relationship between SOC and BSI

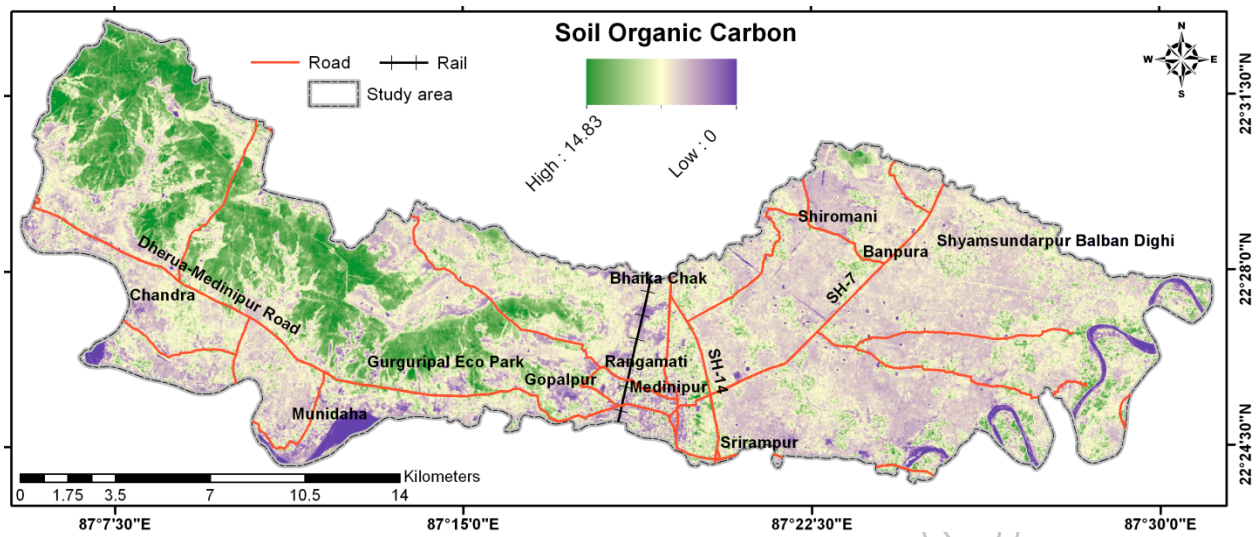

Fig. 5 Digital SOC map of Medinipur Block

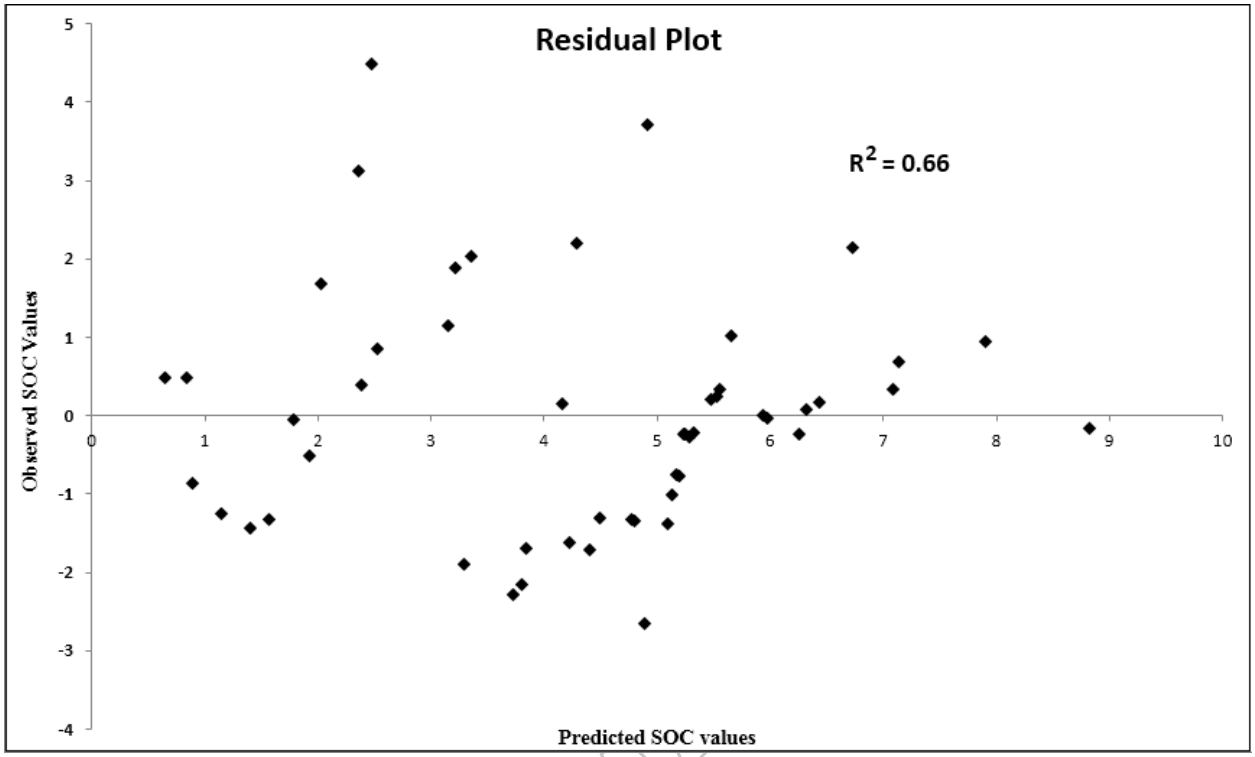

Fig. 6 Residual plot based on the observed and predicted SOC.